International Journal of
Plant Biology

MDPI

Article

Phototrophic Microbial Communities and Root Anatomical Adaptations of the Leafless Epiphytic Orchid *Chiloschista lunifera* (Rchb.f.) J.J.Sm

Anawat Padpaiboon [1], Nuttha Sanevas [1] and Pornsawan Sutthinon [1,2,*]

[1] Department of Botany, Faculty of Science, Kasetsart University, Bangkok 10900, Thailand; anawat.pad@ku.th (A.P.); fscintsv@ku.ac.th (N.S.)
[2] Biodiversity Center, Kasetsart University, Bangkok 10900, Thailand
* Correspondence: pornsawan.sut@ku.th; Tel.:+66-3335-2646

Abstract

Epiphytic and leafless orchids possess specialized root structures and host diverse associated microorganisms, which may contribute to their adaptation to limited access to water, nutrients, and photosynthetic tissues. Microscopic, anatomical, and molecular analyses of aerial and substrate roots of *Chiloschista lunifera* (Rchb.f.) J.J.Sm. revealed consistent phototrophic microbial biofilms on the velamen surface. These biofilms comprised filamentous and unicellular cyanobacteria, singular bacterial cells, and green algae. Morphological characterisation identified cyanobacteria belonging to five taxonomic orders, which are Chroococcales, Chroococcidiopsidales, Nostocales, Leptolyngbyales, and Synechococcales. 16S rRNA amplicon sequencing confirmed cyanobacterial dominance, with *Chroococcidiopsis thermalis* PCC 7203 strongly prevalent in root wash samples (up to 99.99% relative abundance), while root homogenate samples harboured a more diverse assemblage including Phormidiaceae, *Leptolyngbya*, *Scytonema*, and *Calothrix*. In addition, a green alga from Watanabeales (*Jaagichlorella* sp.) was identified based on morphological characteristics. TEM showed diverse cyanobacterial forms and unicellular green algae with well-developed photosynthetic structures. Root anatomy differed between root types. Substrate roots exhibited an inverted kidney-shaped transverse profile, whereas aerial roots were circular, with differences in velamen distribution reflecting adaptation for water retention and substrate attachment. Branched root hairs occurred on substrate roots, while aerial roots possessed unbranched root hairs, indicating functional specialization. Autofluorescence analysis revealed lignified tissues and abundant cortical chloroplasts, suggesting a photosynthetic role of the roots that may compensate for leaflessness. These findings enhance our understanding of the anatomical and ultrastructural features of epiphytic leafless orchid roots and may support future conservation and propagation efforts.

Keywords: cyanobacteria; epiphytic orchids; green algae; root anatomy; velamen

Check for updates

Academic Editor: Zhaoyong Shi

Received: 27 February 2026
Revised: 18 April 2026
Accepted: 20 April 2026
Published: 26 April 2026

Copyright: © 2026 by the authors. Licensee MDPI, Basel, Switzerland. This article is an open access article distributed under the terms and conditions of the Creative Commons Attribution (CC BY) license.

1. Introduction

Chiloschista spp., commonly known as starfish orchids, are a group of epiphytic leafless orchids belonging to the family Orchidaceae [1]. This genus comprises 20 species primarily distributed across the Indian subcontinent and the Himalayas, as well as regions such as China, Taiwan, Thailand, Indonesia, Australia, New Guinea, Fiji, and Micronesia [2]. According to their unique characteristics, *Chiloschista* species are in great demand within the commercial market [3]. Currently, the population of this orchid genus is relatively

limited. Therefore, the species of *Chiloschista* are listed in Appendix II of the Convention on International Trade in Endangered Species (CITES) [4].

Unlike most orchids, leafless species possess highly reduced or absent leaves, relying instead on specialized aerial roots for both water absorption and photosynthesis [5]. To improve water-use efficiency, these orchids utilize Crassulacean Acid Metabolism (CAM), a specialized photosynthetic pathway that allows them to conserve water while still performing photosynthesis [6]. Therefore, their roots perform dual functions: anchorage and photosynthesis.

Moreover, leafless orchids are considered some of the most specialized plants, having coevolved intricately with their biotic partners, especially mycorrhiza. Their tiny seeds lack endosperm, requiring infection by endophytic fungi for germination and early seedling development [7]. In addition to mycorrhizal symbiosis, several studies have reported that the roots of many epiphytic orchids host cyanobacteria or blue-green algae, including *Nostoc*, *Oscillatoria*, *Calothrix*, and *Anabaena* (all belonging to the phylum Cyanobacteria). Generally, plant-associated microorganisms can occupy the root surface, forming complex multicellular and often multispecies assemblies called biofilms [8]. It was also reported that the velamen layer, a multi-layered epidermis in orchid roots, plays a crucial role in retaining moisture and creating favorable conditions for the growth of photoautotrophic algae on the root surface. This results in a green biofilm covering the entire root [9].

Tsavkelova et al. (2022) report that *Chiloschista parishii* Seidenf. host a cyanobacterial community primarily composed of nitrogen-fixing filamentous species from the orders Nostocales, Synechococcales, and Oscillatoriales [10]. Compared to the leafy epiphytic orchids (*Dendrobium moschatum* and *Acampe preamorsa*), the aerial roots of leafless orchids (*Chiloschista parishii* and *Microcoelia moreauae*) were more abundantly colonized by a diverse range of cyanobacteria [10]. In certain filamentous cyanobacteria, they usually convert atmospheric nitrogen (N_2) into ammonia (NH_3), a form of nitrogen that organisms can use for growth through a specialized nitrogen-fixing cell called a heterocyst [11]. Additionally, cyanobacteria associated with orchids have been reported to produce gibberellin, cytokinin, ethylene, abscisic acid, and certain B vitamins [12].

In addition to cyanobacteria, Deepthi et al. (2020) also identified several other green algae, such as *Klebsormidium flaccidum*, *Chlorella* sp., *Myrmecia* sp., *Enallax costatus*, *Chlorococcum minutum*, and *Stichococcus bacillaris*, inhabiting the roots of epiphytic orchids [9]. When comparing nitrogen levels, it was found that orchid root tissues contained significantly higher amounts of nitrogen than leaf tissues [9]. However, studies on the relationships and types of algae inhabiting the roots of orchids in *Chiloschista* are still very limited.

Generally, the roots of epiphytic orchids are found growing in the air, anchored to the bark, or extending into the soil [13]. Several morphological and anatomical adaptations have been observed between aerial roots, terrestrial roots, and substrate roots, exhibiting distinct structural differences that reflect their specialized functions and environmental interactions. For instance, the aerial and terrestrial roots of *Acampe praemorsa* were cylindrical, whereas those in contact with the bark were flattened on the side facing the bark [13]. Root hairs, essential for water and nutrient uptake [14], have been reported to develop only on roots grown in soil or on regions of the roots that were attached to the bark. Moreover, the amount of aerenchyma in roots tends to increase with higher soil moisture levels [13]. Research on the anatomical characteristics of the roots of leafless orchids in relation to algae colonization, as well as the diversity of algae, is essential to confirm the preliminary roles and significance of algae in the roots of leafless orchids.

Chiloschista lunifera (Rchb.f.) J.J.Sm. is an epiphytic orchid found in Thailand, typically in evergreen and mixed deciduous forests in the northern and northeastern regions, particularly in Chiang Mai and Loei provinces (from the curated display of dried specimens at the

Bangkok Forest Herbarium, BKF). Despite the great interest in representatives of the leafless orchid in Thailand, information on root morphological and anatomical characteristics, as well as algal and cyanobacterial diversity in root remains, is underexplored. Understanding their structural adaptations and algal diversity can provide insights into their physiology, ecological interactions, and potential conservation strategies in the future. Therefore, this research aims to assess algal diversity and root anatomical adaptations in *C. lunifera*.

2. Materials and Methods

2.1. Plant Materials

The 4-year-old *C. lunifera* were planted by securing their roots with an orchid planting plastic sheet. They were grown in a greenhouse with 70% shading net with 30–45 °C of temperature and high relative humidity at 45–60% under a 12/12 photoperiod. The irrigation system provided 6 waterings spread across every 4 h for 10 min during the daytime, utilizing an automatic watering system. All plants were cultivated in the greenhouse of the Department of Botany, Faculty of Science, Kasetsart University.

2.2. Root Morphology and Micromorphology

Root samples were collected from four individual plants (biological replicates) of *C. lunifera*. From each plant, three to four healthy, mature roots were randomly selected from two distinct types: (1) substrate roots attached to the planting material, and (2) aerial roots hanging freely. Only visibly healthy roots without disease symptoms or physical damage were collected. Roots were cut using a sterile razor blade and processed immediately for further analysis as described below.

2.2.1. Light Microscope (LM) Observation

Orchid roots with visibly noticeable biofilm were sectioned and examined using a Carl Zeiss Stemi 508 Stereozoom microscope (Carl Zeiss AG, Oberkochen, Germany). Images were captured with an Axiocam ERc 5s camera and processed with ZEN 2 (blue edition) software.

2.2.2. Scanning Electron Microscope (SEM) Observation

Fresh orchid roots with biofilm were cross-sectioned 0.5–1 cm long, divided into upper and lower sides (only the substrate roots), and fixed in SEM fixative (2.5% glutaraldehyde dissolved in 0.1 M phosphate-buffered solution (PBS), pH 7.2) for 30 min. The samples were washed in 0.1 M phosphate buffer (pH 7.2) and subsequently dehydrated through a graded ethanol series (30%, 50%, 75%, 95%, and 100%), followed by a mixed series of absolute ethanol and acetone (3:1, 1:1, and 1:3). Each step was carried out for 1–2 h. Critical Point Drying (CPD) was applied, followed by mounting the dried samples on stubs with double-sided tape. The samples were sputter-coated with gold and examined using an FEI Quanta 450 SEM (FEI Company, Hillsboro, OR, USA).

2.3. Algal Identification

2.3.1. Algae Isolation

Root samples with biofilm from four orchid plants were randomly selected, sterilized, and cut transversely into 1 cm-long segments. The samples were then ground using a mortar and pestle, mixed with distilled water, and incubated in BG-11 medium for 4–5 weeks at room temperature (23–26 °C) under a 12 h light cycle. After 3 months, algae samples were observed using an Olympus BX-53 microscope equipped with a digital camera (Olympus Corporation, Tokyo, Japan).

2.3.2. Morphological Identification of the Algal Associates

Microalgae isolated from the root-associated biofilm and subsequently cultured in nutrient medium were microscopically examined to characterize their detailed morphological features and structural variations. Key features such as the shape and size of vegetative cells, the presence or absence of the sheath, and heterocysts were recorded. Morphological identification was conducted using standard taxonomic manuals [15–19]. Cyanobacterial classification followed the most recent taxonomic treatment adopted in AlgaeBase [20] based on [18], which places the genus *Fischerella* within Nostocales (Hapalosiphonaceae). The green alga was assigned to Watanabeales following [21] and AlgaeBase.

2.3.3. Transmission Electron Microscopy (TEM) Observation

The collected roots with biofilm were immediately fixed in 2.5% glutaraldehyde prepared in 0.1 M phosphate-buffered solution (PBS, pH 7.2) and incubated at room temperature for 3 h. The specimens were rinsed three times in 0.1 M PBS (5 min each) and post-fixed in 1% osmium tetroxide for 1–2 h. After thorough washing with distilled water (DW), they were stained with 5% uranyl acetate for 20 min. Dehydration was performed through a graded ethanol series (70%, 80%, 90%, and 100%; 15 min each), followed by acetone treatment. The stained samples were subsequently embedded and polymerized in epoxy resin (Epon-812; Electron Microscopy Sciences, PA, USA). Resin blocks were trimmed with a razor blade and sectioned using a Leica EM UC7 Ultramicrotome (Leica Microsystems, Wetzlar, Germany). Semi-thin sections (300 nm) were cut with a glass knife, mounted on glass slides, and stained with toluidine blue O in 1% sodium borate for light microscopy (LM). Images were captured using an Olympus BX-53 microscope equipped with a DP74 digital camera (Olympus Corporation, Tokyo, Japan). For ultrastructural analysis, ultra-thin sections (70 nm) were obtained using a diamond knife (DiATOME Ltd., Nidau, Switzerland) on a Leica EM UC7 Ultramicrotome. Sections were mounted on formvar-coated copper grids and contrasted with uranyl acetate for 40 min, followed by lead citrate staining for 3 min (UPb staining). Observations were carried out with a Zeiss EM900 transmission electron microscope (Carl Zeiss AG, Oberkochen, Germany).

2.3.4. DNA Extraction and Quality Assessment

Algae samples incubated in flasks for four months were filtered and transferred into sterile plastic tubes. Total genomic DNA was extracted using the NucleoSpin Plant II kit (Macherey-Nagel, Düren, Germany) following the manufacturer's standard protocol [22], with the final DNA eluted in 50 µL of Buffer PE. The quantity and quality of the extracted DNA were evaluated using a BioPhotometer Plus UV/Vis Photometer (Eppendorf, Hamburg, Germany) with an Eppendorf cuvette g10. The process involved blanking the instrument with 1 µL of Buffer PE, followed by measuring 1 µL of the DNA sample. DNA concentration and the A260/A280 absorbance ratio were recorded to assess purity, targeting a ratio between 1.8 and 2.0 for high-quality genomic DNA.

DNA integrity was further verified via gel electrophoresis using a 1.5% agarose gel in 1X TBE buffer. A volume of 1 µL of 1 kb DNA Ladder mixed with 2 µL of loading dye was loaded into the first well, followed by 1 µL of each DNA sample mixed with 2 µL of loading dye in subsequent wells. Electrophoresis was performed at 100 V for 20 min, and the resulting bands were visualized under UV light. Validated DNA samples were submitted to the Kasetsart University (KSGtEC), Faculty of Science, for library preparation and sequencing.

2.3.5. Library Preparation and Sequencing

Cyanobacterial community composition was assessed by targeting the 16S rRNA gene region. Target amplification was performed using specific primers: C_773F (5′–AAW GGG ATT AGA TAC CCC WGT–3′) and C_1200R (5′–RGG KTG CGC TCG TTG CGG GA–3′). Libraries were generated using the Salus 16S Detection Library Preparation Kit (Salus Biotechnology Co., Ltd., Shanghai, China) following a two-step PCR strategy, which included initial target amplification followed by dual indexing.

Following amplification, the amplicons were purified using a magnetic bead-based cleanup system. The resulting libraries were quantified using the Qubit dsDNA High Sensitivity Assay (Thermo Fisher Scientific, Waltham, MA, USA). Library normalization was performed through equimolar pooling based on the molarity of each sample. Sequencing was conducted on the Salus PE300 platform (Salus Biotechnology Co., Ltd., Shanghai, China) using a paired-end 2 × 300 bp configuration.

2.3.6. Taxonomic Analysis and Bioinformatics

Raw sequencing data in FASTQ format were processed through a bioinformatics pipeline starting with quality control (QC) assessment using FastQC Version 0.12.1, with overall summaries generated by MultiQC. Adapter sequences and low-quality bases were trimmed using Cutadapt Version 4.6 to refine the dataset. High-quality reads were then analyzed using the DADA2 algorithm, which performed error correction, read merging, and chimera removal to identify Amplicon Sequence Variants (ASVs). Taxonomic assignment was conducted by comparing ASV sequences against the SILVA reference database (version 138.2) using QIIME 2, applying a minimum bootstrap confidence threshold of 50. Taxa assigned below this threshold were reported at the next higher taxonomic rank. Given the limited representation of epiphytic and freshwater cyanobacterial diversity in the SILVA 138.2 reference database, genus-level resolution was not achievable for all taxa; assignments are therefore reported at the lowest reliably resolved rank. Strain-level designations reflect the closest reference matches within the database and should be interpreted as putative identifications rather than confirmed strain identities.

2.4. Root Anatomy

To investigate the anatomical characteristics of the leafless orchid roots, fresh aerial and substrate roots were collected from three individual plants (as biological replicates) and processed using free-hand sectioning, followed by safranin and fast green staining, and observed under a light microscope (LM). Anatomical features, including velamen layers, exodermis wall thickening, number of cortex layers, endodermal cell wall thickening, and vascular bundle arrangement, were documented. Photos were taken using an Olympus BX-53 microscope equipped with a DP74 digital camera (Olympus Corporation, Tokyo, Japan).

2.5. Lignin and Chloroplast Localization

Fresh root samples were transversely sectioned using freehand sectioning. Lignin and chloroplast localization were examined in the cross-sections using a DAPI filter (excitation at 358 nm; emission at 461 nm). Photographs were captured with an Olympus BX-53 microscope with a DP74 digital camera (Olympus Corporation, Tokyo, Japan).

3. Results

3.1. Root Morphology and Micromorphology

Chiloschista lunifera is a monopodial orchid with an epiphytic habit. It possesses clinging roots for anchorage (substrate roots) and aerial roots that hang freely in the air

(Figure 1A). The roots of the orchids were usually green. Examination under a stereomicroscope revealed that the dorsal side of the roots was predominantly covered with a biofilm, particularly at the base of the root (Figure 1B). Biofilm was characterized by a thick light green tone (Figure 1B). The number of roots per plant varied from 13 to 18 roots, and the average root length was 15.56 ± 5.069 cm. SEM observations of the root surface confirmed the presence of microorganisms, with both unicellular and filamentous forms of algae detected on the velamen of aerial roots (Figure 2A,B, arrowheads) and substrate roots. On the dorsal surface of the substrate root, a biofilm with algal communities was shown (Figure 2C). In contrast, no algal communities were observed on the ventral surface (Figure 2D). Moreover, velamen, especially on the ventral side of the substrate root, possessed reticulated cell wall thickening (Figure 2E,F).

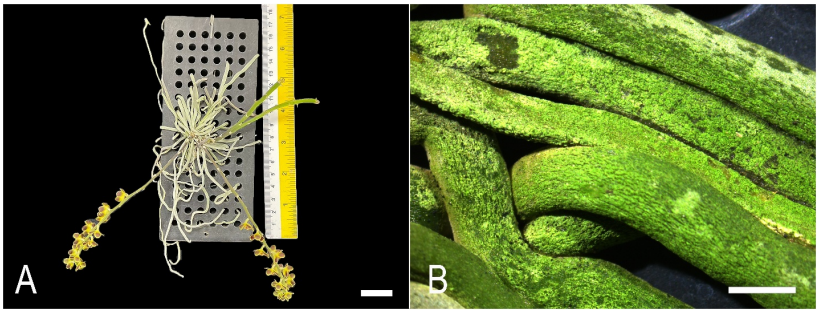


Figure 1. Root morphology and biofilm region on *C. lunifera* root surface (**A**) An epiphytic *C. lunifera* anchoring to a planting plastic sheet. (**B**) A densely packed biofilm on the root surface. Scale bars. (**A**) = 2.54 cm; (**B**) = 0.5 mm.

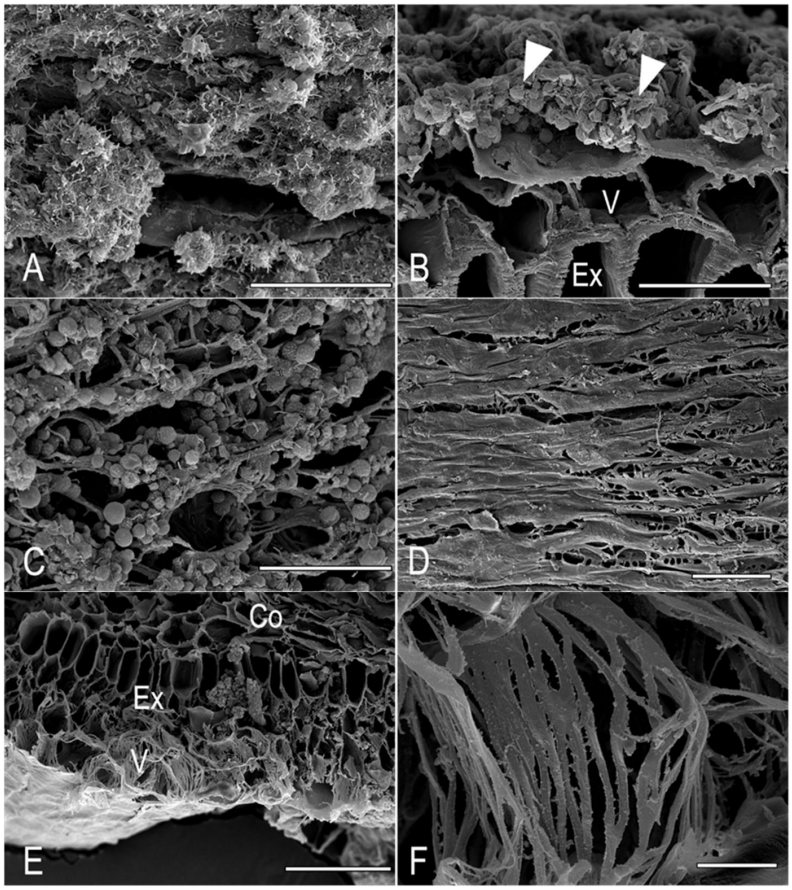


Figure 2. SEM micrographs of *C. lunifera* root. (**A**) Biofilm composed of an algal community on the velamen surface of the aerial root. (**B**) Biofilm attached to the dorsal side (arrowheads) of the aerial

root. (**C**) Unicellular and filamentous forms of algae on the velamen of substrate roots. (**D**) The ventral surface of the substrate root lacked an algal community. (**E**) Cell wall thickening of velamen on the ventral side of the substrate root. (**F**) Magnified view of reticulated cell wall thickening of velamen. Abbreviations: Co, cortex; Ex, exodermis; V, velamen. Scale bars. (**A**–**C**) = 50 µm; (**D**) = 100 µm; (**E**,**F**) = 10 µm.

3.2. Algal Observation

Algal isolation procedures followed by light microscopic examination revealed abundant root unicellular algal aggregates and filamentous forms within the biofilms. Morphological characterization identified cyanobacteria representing five distinct taxonomic orders: Chroococcales (*Chroococcus* sp., Figure 3A, arrowhead), Chroococcidiopsidales (*Gloeocapsa* sp., Figure 3B, arrowhead), Nostocales (*Nostoc* sp. and *Fischerella* sp., Figure 3C,E, arrowheads), Leptolyngbyales (*Leptolyngbya* sp., Figure 3D, arrowhead), and Synechococcales (*Synechococcus* sp., Figure 3E, red arrowhead). Classification followed [18] as adopted in AlgaeBase [20]. Microscopic observations indicated that members of Nostocales were the most frequently encountered cyanobacterial group among the cultured isolates obtained from the biofilm community. Additionally, a green alga, *Jaagichlorella* sp. (Watanabeales, Trebouxiophyceae; [21]), was identified based on morphological characteristics (Figure 3F, arrowhead). Molecular confirmation was not achievable within the 16S rRNA framework applied in this study, as this marker does not target eukaryotic taxa.

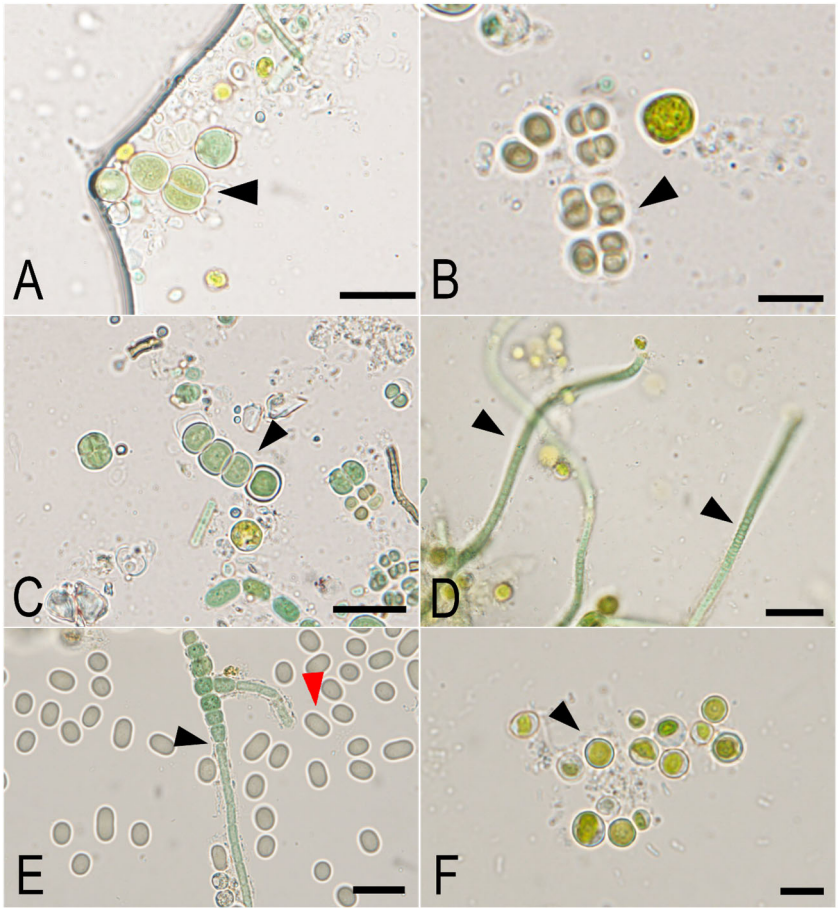


Figure 3. Light micrographs of cyanobacteria and green algae isolated from the biofilm of aerial and substrate roots of *C. lunifera*. Arrowheads point to the target cyanobacteria or green algae described. (**A**) *Chroococcus* sp. (**B**) *Gloeocapsa* sp. (**C**) *Nostoc* sp. (**D**) *Leptolyngbya* sp. (**E**) *Fischerella* sp., and *Synechococcus* sp. (red arrowhead), (**F**) *Jaagichlorella* sp. Scale bars. (**A**) = 10 µm; (**B**) = 5 µm; (**C**–**E**) = 10 µm; (**F**) = 5 µm.

3.3. Transmission Electron Microscopy (TEM) Observation

TEM micrographs displayed the cellular ultrastructure of cyanobacterial cells. Singular cell (Figure 4A), colonial form (Figure 4B,C) and filamentous form (Figure 4D) were found. The cells were bounded by a distinct multilayered cell envelope. Small vacuoles were observed as electron-transparent, membrane-bound compartments dispersed within the cytoplasm (Figure 4E). The cytoplasm was densely packed with parallel arrays of thylakoid membranes distributed throughout the peripheral region of the cell, indicating active photosynthetic capacity (Figure 4F).

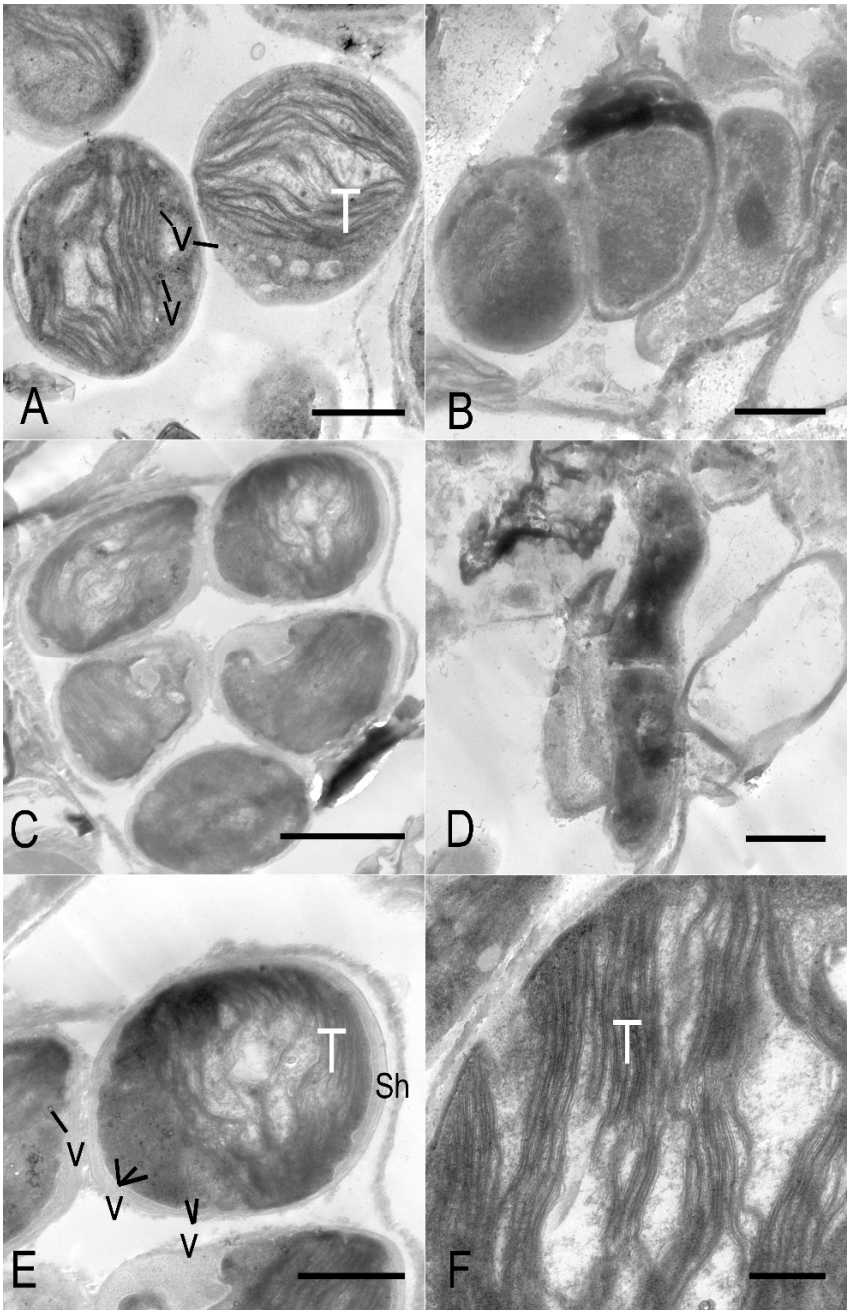


Figure 4. TEM micrographs of cyanobacteria found in the biofilm of *C. lunifera* roots. (**A**) Unicellular cyanobacteria. (**B**) Colonial 2-cell cyanobacteria. (**C**) Colonial 5-cell cyanobacteria. (**D**) Filamentous cyanobacteria. (**E**) Ultrastructure of cyanobacterial cells showing thylakoids, sheath, and vesicle. (**F**) Magnified view of parallel arrays of thylakoids of cyanobacteria. Abbreviations: Sh, sheath; T, thylakoids; V, vesicle. Scale bars. (**A**) = 1 μm; (**B**) = 500 nm; (**C**) = 2 μm; (**D**) = 500 nm; (**E**) = 1 μm; (**F**) = 500 nm.

Meanwhile, the unicellular green algae cells were enclosed by a well-defined cell wall and externally surrounded by an extracellular sheath, which appeared as an electron-lucent to moderately electron-dense layer of variable thickness. The cytoplasm contained a prominent nucleus and a single chloroplast occupying a large portion of the cell periphery. Within the chloroplast, thylakoids were arranged in parallel arrays. A distinct pyrenoid was observed within the chloroplast and was frequently associated with adjacent starch grains (Figure 5). Moreover, electron-dense globular droplets were also detected within the pyrenoid (Figure 5, arrowheads). In addition, discrete lipid droplets were present in the cytoplasm as rounded inclusions (Figure 5).

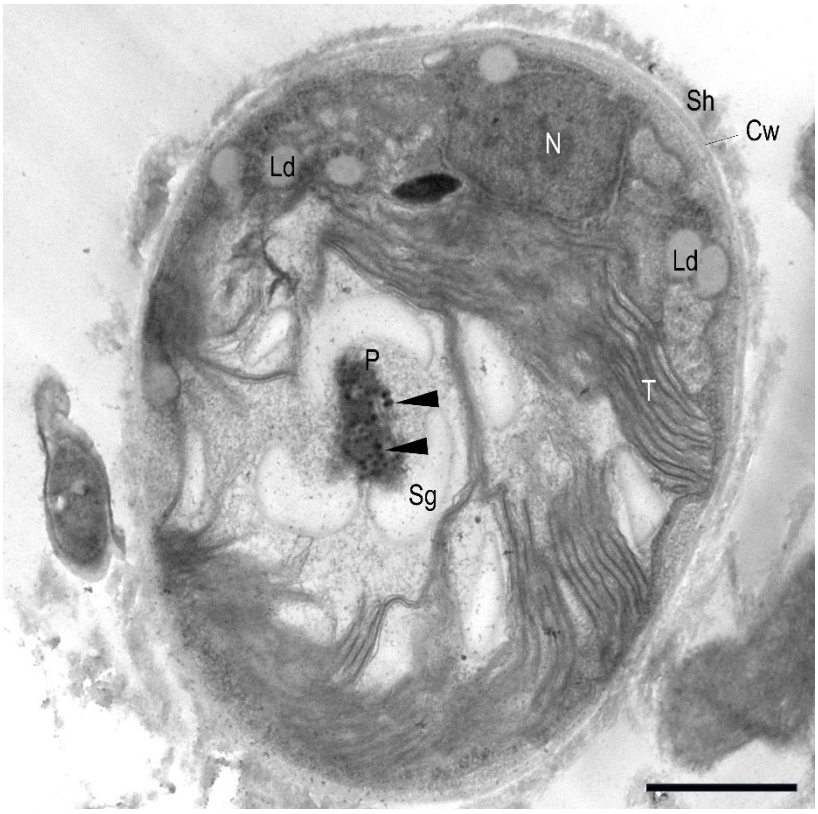


Figure 5. TEM micrographs of green algae found in the biofilm of *C. lunifera* roots, showing a prominent pyrenoid encircled by electron-dense globular droplets (arrowheads). Abbreviations: Cw, cell wall; Ld, lipid droplet; N, nucleus; P, pyrenoid; Sh, sheath; Sg, starch grain; T, thylakoids. Scale bar = 1 μm.

3.4. Cyanobacterial Community Composition Based on 16S rRNA Amplicon Sequencing

The 16S rRNA amplicon sequencing identified the cyanobacterial community as primarily comprising *Chroococcidiopsis thermalis*, members of the family Phormidiaceae, and *Leptolyngbya*. In particular, the root wash samples were consistently dominated by *Chroococcidiopsis thermalis* PCC 7203, whereas the root homogenate samples exhibited a more variable composition, including Phormidiaceae, *Leptolyngbya*, *Scytonema* strain UCFS19, and *Calothrix* (Figure 6). Detailed quantification across the root homogenate samples (S1–S4) and root wash samples (W1–W4) further elucidated this taxonomic distribution. In the root homogenate group, sample S1_16S yielded 111,030 total reads and was characterized by a high prevalence of the family Phormidiaceae at 79.50%, followed by *C. thermalis* at 17.77%, while the genus *Aliterella* and family Chroococcidiopsaceae were present in negligible amounts. In contrast, sample S2_16S, despite a lower read count of 4305, maintained a core population of *C. thermalis* PCC 7203 at 38.40%, supplemented by Phormidiaceae at 11.96% and *Leptolyngbya* sp. strain ANT.L52.2 at 9.04%, with minor contributions from *Scytonema*

strain UCFS19 and *Calothrix* strain PCC-6303. This variability in the homogenate group was also evident in sample S3_16S, which recorded 98,179 reads and a 11.28% abundance of *C. thermalis* PCC 7203, and reached an extreme in sample S4_16S, where *Leptolyngbya* sp. strain ANT.L52.2 became the overwhelmingly dominant taxon at 94.87% of the 110,294 reads obtained.

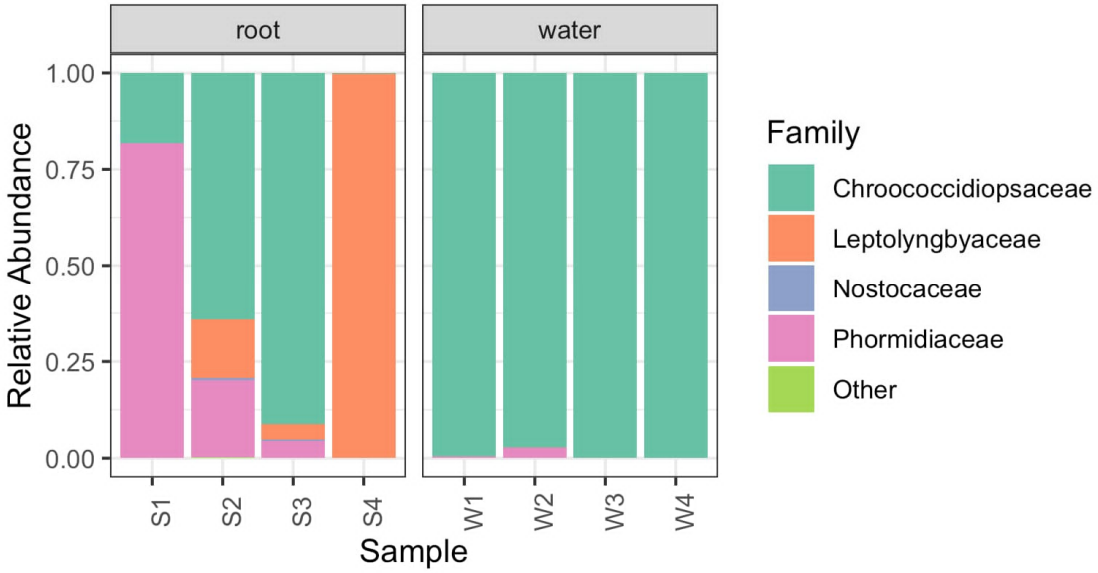


Figure 6. Relative abundance of Cyanobacteria genera in liquid medium from root wash samples (W1–W4) and root homogenate samples (S1–S4) based on 16S rRNA gene sequencing.

Conversely, the root wash samples (W1–W4) exhibited a much higher degree of taxonomic uniformity, consistently showing the strong establishment of *C. thermalis* PCC 7203 on the external velamen surface. Sample W1_16S and W2_16S displayed 77.93% and 87.12% abundance of this species, respectively, with Phormidiaceae remaining the primary secondary group. The dominance of *C. thermalis* PCC 7203 became nearly absolute in the remaining samples, reaching 99.39% in W3_16S and an exceptional 99.99% in W4_16S, suggesting that this particular strain is highly adapted to the microenvironment of the *C. lunifera* root surface. These results indicate that while the external biofilm is largely a monoculture of *Chroococcidiopsis*, the internal or more tightly adhered microbial communities within the root tissues harbor a more diverse assemblage of cyanobacterial functional groups, potentially reflecting different ecological niches and physiological roles within the orchid-microbe association.

3.5. Anatomical Observation

Based on the anatomical observation, transverse sections of the substrate roots of the investigated species resemble an inverted kidney shape, with a distinct dorsal and ventral side. The dorsal side, which faces away from the substrate, appears more convex, while the ventral side, in contact with the substrate, is slightly concave (Figure 7A). Roots are typically covered with 2–3 layers of velamen in the ventral side (Figure 7B). The velamen secondary cell wall thickening is reticulated (Figure 7C, arrowhead). Branched root hairs are also found in the ventral portion (Figure 7D). However, at the dorsal region of the root, only a single epidermal layer is present, with no velamen. Next to the velamen, an uniseriate exodermis with U-shape thickening of cell walls was shown (Figure 7E). Cortex usually composed of 8–12 layers of parenchyma. Aerenchyma cells are primarily found along the dorsal cortex (Figure 7F, arrowheads). Raphide crystals were also seen in some aerenchyma (Figure 7G, arrowhead). Steles with a single vascular cylinder, usually polyarches with

5–6 xylem arches, surrounded by an O-thickening endodermis, interrupted by 1–3 cells of thin-walled passage cells. Pith was mainly sclerenchyma (Figure 7H).

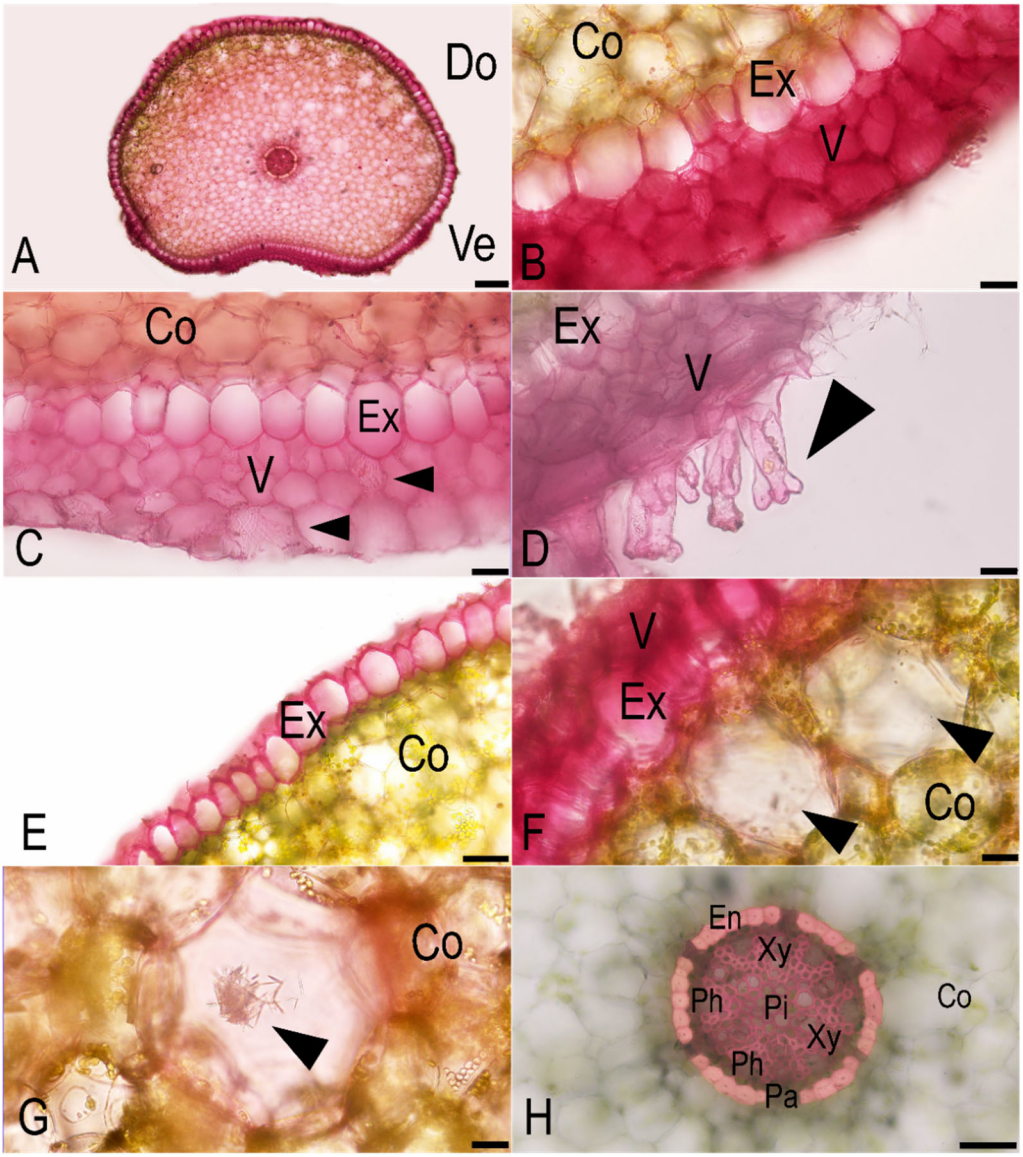


Figure 7. Anatomical characters of substrate root in *C. lunifera*. (**A**) An overview of the substrate root cross-section. (**B**) Velamen' ventral side. (**C**) Exodermis with reticulate cell wall thickening (arrowheads). (**D**) Branched root hairs developing from the velamen on the ventral side (arrowheads). (**E**) Non-velamen' dorsal side. (**F**) Aerenchyma in cortex (arrowheads). (**G**) Raphide crystal in cavity (arrowhead). (**H**) Stele showing obvious endodermis with a thick wall surrounding vascular tissue. Abbreviations: Co, cortex; Do, dorsal side; En, endodermis; Ex, exodermis; Pa, passage cell; Ph, phloem; Pi, pith; V, velamen; Ve, ventral side; Xy, xylem. Scale bars. (**A**) = 200 µm; (**B**–**D**) = 20 µm; (**E**) = 50 µm; (**F**–**G**) = 20 µm; (**H**) = 50 µm.

According to an anatomical examination, the transverse section roots of aerial roots of *C. lunifera* were round in shape (Figure 8A). Roots were typically covered with 2–3 layers of velamen (Figure 8B). Root hairs were abundant only on one side (Figure 8C). The cell wall thickening of velamen was reticulated and elliptical (Figure 8D, arrowhead). The exodermis is a single-layered, cylindrical structure with U-form thickening walls (Figure 8E). The cortex typically consisted of 9–13 layers of parenchyma. Aerenchyma was also present within the cortex (Figure 8F, arrowheads), with some containing raphide crystals (Figure 8G,

arrowhead). The endodermis was distinctly characterized by O-shaped cell wall thickening, interrupted by 1–2 passage cells, with the pith also composed of sclerenchyma (Figure 8H).

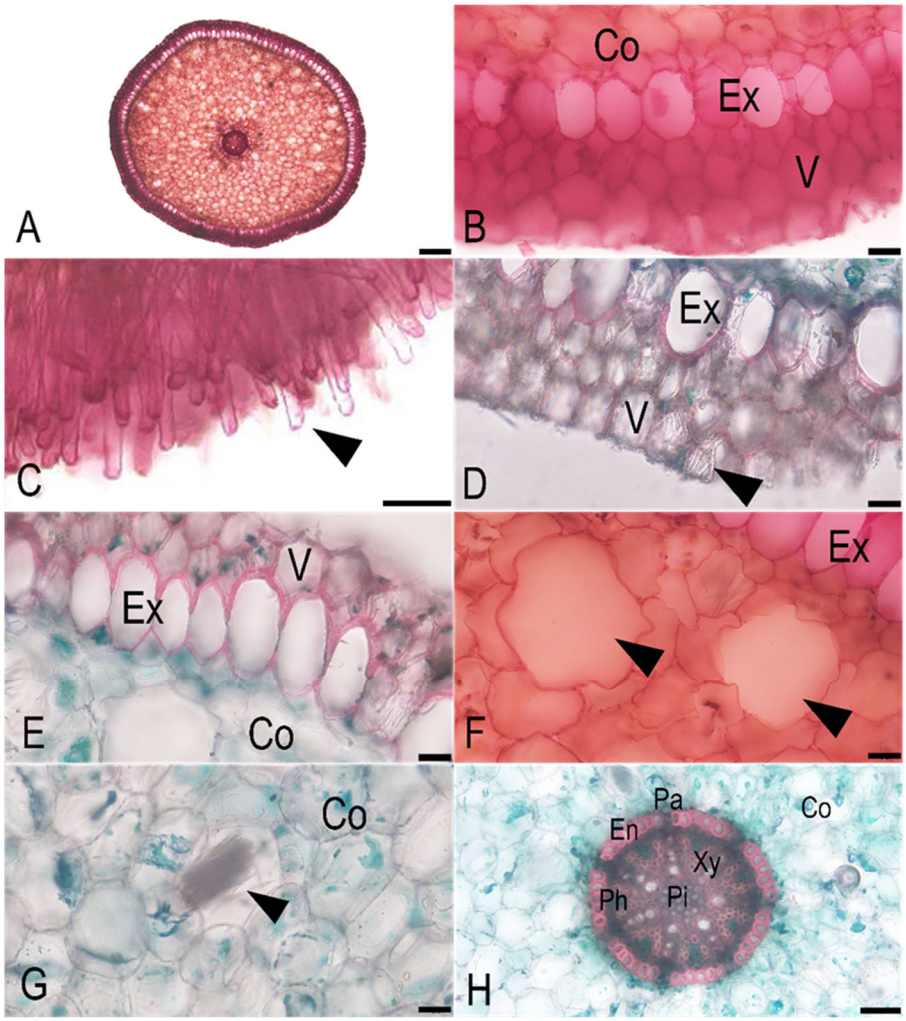


Figure 8. Anatomical characters of aerial root in *C. lunifera*. (**A**) An overview of the aerial root cross-section. (**B**) Velamen layers with exodermis. (**C**) Root hairs developing from one side of the root (arrowhead). (**D**) The reticulate cell wall thickening of a velamentous cell (arrowhead). (**E**) Exodermis with U-shaped wall thickening. (**F**) Cavity in cortex (arrowheads). (**G**) Raphide crystals in cavity (arrowhead). (**H**) Stele with endodermis surrounding vascular tissue and sclerchymatous pith. Abbreviations: Co, cortex; En, endodermis; Ex, exodermis; Pa, passage cell; Ph, phloem; Pi, pith; V, velamen; Xy, xylem. Scale bars. (**A**) = 200 µm; (**B**) = 20 µm; (**C**) = 50 µm; (**D**–**G**) = 20 µm; (**H**) = 50 µm.

Lignified tissues and chloroplasts were detected by autofluorescence analysis using a DAPI filter. Lignin was blue, and the chloroplasts appeared red under the fluorescence microscope. On the velamen surface, the biofilm exhibited a positive chloroplast signal (Figure 9A). Chloroplasts were also detected in the exodermis (Figure 9B). Lignin impregnation was detected in the exodermis of both aerial root and substrate root (Figure 9C). However, the exodermis presented a distinct accumulation pattern. Lignin in the substrate root was thin with O-form thickening (Figure 9D), while the aerial root exhibited U-form thickening. The whole cortex is photosynthetic, with a higher chloroplast concentration compared to velamen and pith (Figure 9C). The strongest signal of lignin was detected in the thick wall of endodermis, and some sclerenchyma cells in pith (Figure 9E). Meanwhile, the passage cells lacked lignin in their walls (Figure 9F).

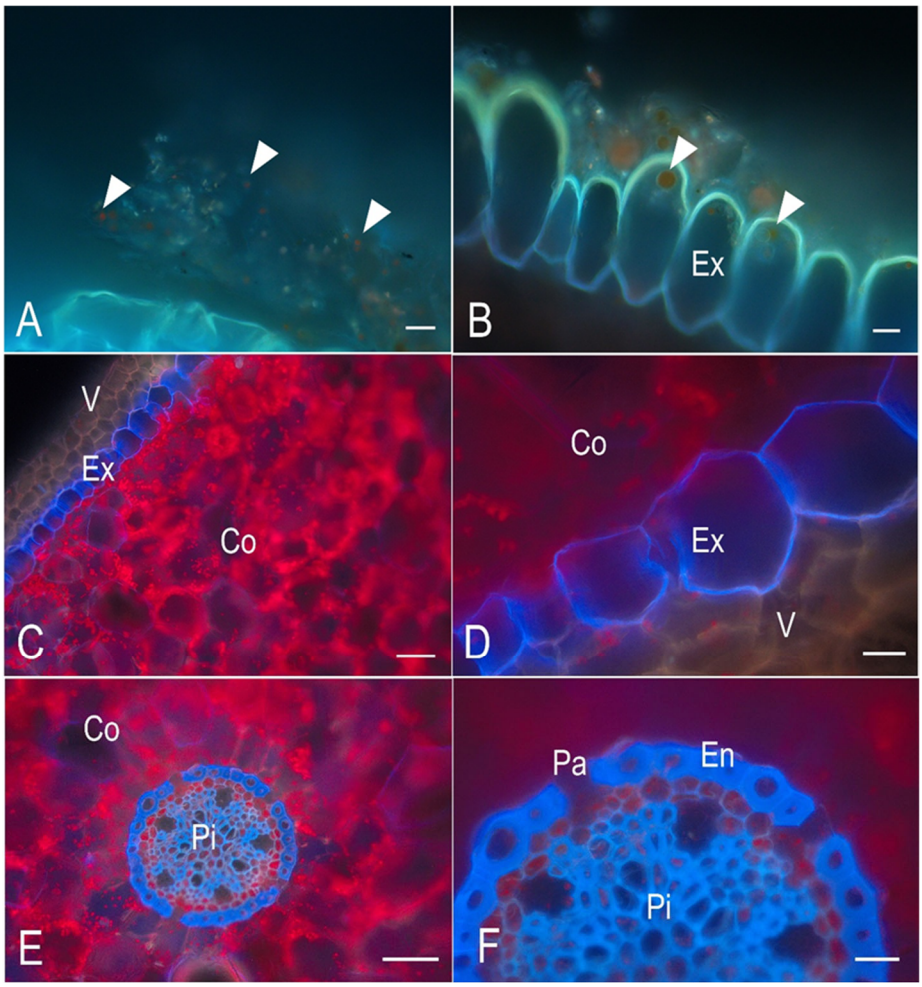


Figure 9. Autofluorescence micrographs using a DAPI filter in the root cross-section of *C. lunifera*. (**A**) The biofilm exhibited a positive chloroplast signal (arrowheads). (**B**) Chloroplast detected in the exodermis (arrowheads). (**C**) Lignin in the exodermis exhibited blue fluorescence, while the abundant chloroplasts appeared red in the cortex. (**D**) The thin lignin in the substrate root exhibiting O-form thickening. (**E**) The strongest lignin signal in the endodermis and sclerenchyma cells of the pith. (**F**) The thick lignified wall of endodermis and the absence of lignin in the passage cells. Abbreviations: Co, cortex; En, endodermis; Ex, exodermis; Pa, passage cell; Pi, pith; V, velamen. Scale bars. (**A**–**F**) = 20 μm.

4. Discussion

The microscopic analysis of both aerial and substrate roots confirmed the occurrence of phototrophic microorganisms on the root surface as biofilm. Both filamentous cyanobacteria and singular cyanobacterial cells were found on the velamen surface. The present study revealed a diverse cyanobacterial community comprising five taxonomic orders (Chroococcales, Chroococcidiopsidales, Nostocales, Leptolyngbyales, and Synechococcales) associated with orchid root biofilms. Among the cultured isolates, members of Nostocales were the most frequently encountered cyanobacterial group. The 16S rRNA amplicon sequencing revealed that the cyanobacterial community was primarily represented by *Chroococcidiopsis thermalis*, Phormidiaceae, and *Leptolyngbya*, with root wash samples showing near-exclusive dominance by *Chroococcidiopsis thermalis* PCC 7203 (up to 99.99% relative abundance), whereas root homogenate samples harboured a more diverse assemblage. Additionally, one green alga belonging to the order Watanabeales (*Jaagichlorella* sp.) was identified based on morphological characteristics, but was not recovered by molecular analysis.

The concordance between morphological characterization and 16S rRNA amplicon sequencing at the ordinal level mutually corroborates the taxonomic framework presented here. However, the two approaches yielded different patterns of dominance: Nostocales were most prevalent among cultured isolates, whereas *Chroococcidiopsis thermalis* (Chroococcidiopsidales) dominated root wash samples in the sequencing data. This discrepancy is consistent with well-documented cultivation bias toward fast-growing filamentous morphotypes, which are disproportionately recovered under standard culture conditions relative to slow-growing colonial or coccoid forms. The integration of culture-based and culture-independent methods is therefore essential for the comprehensive characterization of orchid root microbial communities.

The limited genus-level resolution for some cyanobacterial taxa in the 16S dataset is consistent with the known underrepresentation of freshwater and epiphytic cyanobacteria in the SILVA 138.2 reference database [23]. Genus- and species-level assignments reflect the closest reference matches and should be regarded as putative identifications; strain-level designations do not constitute confirmed strain identities. The substantially lower read count in sample S2_16S (4305 reads) compared with other samples (>98,000 reads) may have reduced the reliability of relative abundance estimates for this sample and warrants cautious interpretation. The contrasting community compositions between root wash and root homogenate samples suggest that the external velamen surface and the more tightly adhered internal biofilm represent distinct ecological niches. The near-monoculture of *Chroococcidiopsis thermalis* PCC 7203 on the external surface suggests strong niche specialization, possibly facilitated by desiccation tolerance and adaptation to high irradiance on the exposed velamen. In contrast, greater compositional diversity within root homogenate samples may reflect the more stable microhabitat provided by inner velamen layers, where moisture is retained for longer periods.

The discrepancy between morphological identification and molecular analysis is a recognized challenge in phycological studies [24]. This incongruence often stems from phenotypic plasticity, where microalgae exhibit significant morphological transitions in response to environmental stimuli such as light intensity, nutrient availability, or chemical cues from predators. For instance, genera like *Scenedesmus* or *Desmodesmus* can develop protective spines and form colonies in the presence of *Daphnia* (predation pressure) but revert to spineless unicellular forms under predator-free conditions or heavy metal stress [25,26]. Other contributing factors include the limitations of public sequence databases [27] and convergent evolution, where phylogenetically distant taxa evolve similar morphotypes under comparable environmental pressures [28]. Consequently, an integrative taxonomic approach—combining high-resolution microscopy, multilocus genetic analysis, and ecological or biochemical data—is essential to resolve these taxonomic ambiguities and ensure accurate species identification [24].

The diversity of root-associated phototrophic microorganisms observed in this orchid is consistent with recent studies reporting the widespread occurrence of cyanobacteria associated with orchids and their ecological significance. Phototrophic microorganisms have been observed on the velamen of aerial and substrate roots in *Acampe papillosa*, *Dendrobium moschatum*, *Phalaenopsis amabilis*, and *Dendrobium phalaenopsis*, and this study is the first to report the formation of a sheath composed of cyanobacteria [29]. Moreover, studies on the tropical epiphytic orchids have reported cyanobacterial associations in four epiphytic orchid species: *Acampe praemorsa*, *Rhynchostylis retusa*, *Epidendrum radicans*, and *Oncidium sphacelatum* [9]. A total of 24 algal species were isolated from their velamen roots, with the majority identified as cyanobacteria, and many of these belonged to well-known nitrogen-fixing groups. Recently, nitrogen-fixing cyanobacteria forming biofilms on the aerial roots of leafless epiphytic orchids, such as *Microcoelia moreauae* and *Chiloschista*

parishii, have been reported [10]. These microbial communities are dominated by members of the orders Oscillatoriales, Synechococcales, and Nostocales, with community composition varying depending on nitrogen availability. Under nitrogen-limiting conditions, *Leptolyngbya* sp. and *Komarekiella* sp. were found to be predominant [10]. These findings suggest that cyanobacteria may play a significant role in supporting nitrogen nutrition in epiphytic orchids. The present study addresses this gap by applying both morphological characterization and 16S rRNA amplicon sequencing to *Chiloschista lunifera* (Rchb.f.) J.J.Sm., providing a more comprehensive characterization of its root-associated cyanobacterial communities than culture-based methods alone. In addition to the cyanobacteria, green algae belonging to the genus *Jaagichlorella* were found in our study. *Jaagichlorella* sp. is commonly found across diverse habitats, including extreme environments such as desert soil crusts, acidic soils, and even artificial substrates like building surfaces [30]. The velamen roots of epiphytic orchids have been known to provide a unique microenvironment that supports the growth and proliferation of rare and potentially novel microalgal species [31]. The presence of green algae associated with the velamen of orchid roots has been documented in *Acampe praemorsa*, *Acampe papillosa*, *Microcoelia moreauae*, *Spathoglottis plicata*, *Chiloschista parishii*, *Rhynchostylis retusa*, *Phalaenopsis amabilis*, *Epidendrum radicans*, *Dendrobium moschatum*, *Oncidium sphacelatum*, *Dendrobium phalaenopsis* [9,10,29,32–34], *Vanda ampullacea*, *Vanda denisoniana*, and *Vanda bensonii* [31]. These microorganisms are commonly associated with the outer root surface, particularly the velamen, which may provide a suitable habitat due to its exposed, porous, and periodically moistened nature. The proliferation and ecological success of these microalgae on aerial roots reflect their adaptations to desiccation and low-nutrient environments [31]. Although these algae are not known to colonize internal root tissues or form true endosymbiotic associations comparable to mycorrhizal fungi [9], their occurrence on orchid roots suggests that root surface anatomy may play an important role in structuring epiphytic microbial communities. The identification of *Jaagichlorella* sp. based solely on morphological characteristics highlights a limitation of the present molecular framework. Because the 16S rRNA marker targets prokaryotes exclusively, eukaryotic green algae associated with orchid roots cannot be detected or confirmed using this approach. Future studies should employ 18S rRNA or rbcL sequencing to enable species-level molecular characterization of the green algal component of orchid root biofilms, which would also facilitate taxonomic comparison across orchid species and geographic regions. The presence of unicellular or colonial (*Chroococcus*, *Gloeocapsa*) and filamentous forms (*Nostoc*, *Leptolyngbya*, *Fischerella*) in our study reflects the morphological diversity characteristic of cyanobacterial communities in specialized habitats. Cyanobacteria can occur as planktonic cells or form phototrophic biofilms and are found in almost every terrestrial and aquatic habitat, including temporarily moistened rocks and bare soil. The velamen environment appears to provide favorable conditions for both morphological types, supporting complex community structures [35,36]. Root anatomical analysis further showed clear differences between substrate and aerial roots. Substrate roots exhibited an inverted kidney-like shape, whereas aerial roots were generally round. Similar root dimorphism has been reported in *Acampe praemorsa* (Rox.) Blatt. & McCann, where roots in contact with the substrate were flattened on the side adjacent to the bark [37]. This creates a difference in the number of velamen layers between the ventral and dorsal sides of the substrate root. The presence of 2–3 layers of velamen on the ventral side helps retain moisture for longer periods [38]. Meanwhile, the absence of velamen on the flattened dorsal side of the root, likely aiding in firm attachment, is consistent with the observations reported by Tay et al. (2021) [39] in the epiphytic orchid *Epidendrum nocturnum* Jacq. This asymmetry may influence microbial colonization by creating contrasting microhabitats: the velamen-bearing side may favor

microbial persistence through improved moisture retention, while the flattened dorsal side may be more specialized for mechanical attachment to the substrate.

The variation in the number of velamen layers usually reflects differences in environmental conditions. Orchids growing in dry habitats typically develop multiple velamen layers, whereas those found in humid environments usually have no velamen or possess only one to two layers [40,41]. Moreover, the velamen layer in the aerial roots of epiphytic orchids is typically thicker than that of terrestrial orchids, reflecting its role in water absorption and nutrient uptake [42]. In an epiphytic lifestyle, the roots not only function to absorb nutrients and water but also to provide stability to the plant [43]. The secondary cell wall thickening observed in the velamen is another feature that reflects its adaptation to the root's environment. Although these wall thickenings are nearly unique to orchid roots, similar patterned cell walls have also been observed in the roots of various other plant families, including ferns such as *Asplenium* [44] and related species [45]; members of the Cyperaceae and Velloziaceae [46]; and other monocotyledons [47] in [48]. These secondary thickenings of the velamen wall consist of cellulose microfibrils, and their formation is known to be controlled by microtubules [48,49].

Interestingly, we found the branched root hairs on the ventral side of the substrate root, contrasted with normal (unbranched) root hairs on the same side of aerial roots. This agrees with previous reports in which root hairs were observed in areas of direct substrate contact [13,50]. Moreover, the occurrence of branched root hair is in line with the observations in the substrate roots of epiphytic orchid *Luisia tenuifolia* Blume and *Schoenorchis nivea* (Lindl.) Schltr. [51,52]. This indicates functional differentiation in root types. Substrate roots are in direct contact with the substrate surface, where increased surface area provided by branched root hairs may enhance anchorage and absorption of water and nutrients from surface moisture, debris, or microbial biofilms [39]. In contrast, aerial roots are primarily exposed to the air and rely on their velamen tissue for moisture absorption from humidity and rainfall [53]. The presence of unbranched root hairs in aerial roots may reflect a reduced need for intense substrate interaction and instead support basic physiological functions such as limited nutrient uptake or microbial interaction [52]. These differences represent an adaptive strategy of epiphytic orchids to optimize resource acquisition in varying microenvironments.

Lignified tissues and chloroplasts were detected by autofluorescence analysis using a DAPI filter. Chloroplasts were occasionally observed in the biofilm, while they were abundantly present in the cortex. This finding suggests that the root cortex may play a photosynthetic role, compensating for the absence of leaves, similar to what has been observed in other leafless orchids such as *Dendrophylax lindenii* (Lindl.) Benth. ex Rolfe [54]. The exodermis and endodermis consist of specialized cells that develop Casparian strips along their anticlinal walls, serving as protective barriers that regulate and safeguard the cortical regions [55,56]. The Casparian strips are primarily composed of lipid-rich suberin; therefore, the exodermis and endodermis function as bidirectional barriers that regulate and restrict the movement of water and nutrients toward the vascular cylinder [56,57]. The detection of both lignin and chloroplast autofluorescence highlights the dual physiological roles of the roots—mechanical support and photosynthesis.

In contrast to natural epiphytic habitats where orchids are subjected to greater environmental fluctuations, such as variable light intensity, temperature extremes, and periodic desiccation [38,58], the plants used in this study were cultivated under greenhouse conditions (70% shading, 30–45 °C, high relative humidity of 45–60%, and regular watering). Although microbial colonization patterns are known to be susceptible to abiotic variables like humidity and light availability, these controlled circumstances may have affected the biomass and composition of the phototrophic microbial communities colonizing the root

surfaces [10,36,59]. As a result, the cyanobacterial and algal diversity described here might not accurately reflect the communities found in *C. lunifera* wild populations. However, in controlled conditions, our study offers the first baseline data on the presence of microbial communities and root structural adaptations of this leafless orchid, which can serve as a basis for subsequent comparative studies in natural habitats. To verify the ecological importance of these plant-microbe interactions and determine whether comparable communities exist in natural environments, field research is required.

5. Conclusions

The consistent occurrence of diverse phototrophic biofilms, including multiple cyanobacterial orders and green algae on the velamen surface, confirms that the root exterior may serve as a selective and potentially nutritionally significant microhabitat. The observed differences between aerial and substrate roots, particularly in transverse section, velamen distribution, and root hair morphology, reflect clear functional specialization related to water retention, substrate attachment, and environmental adaptation. Furthermore, the presence of lignified tissues and abundant cortical chloroplasts supports the compensatory photosynthetic role of the roots in this leafless orchid. These findings underscore the functional integration of root anatomy and microbial communities in epiphytic, leafless orchids and provide important anatomical and microbiological insights for future conservation and propagation strategies.

Author Contributions: Conceptualization, P.S., A.P. and N.S.; methodology, P.S., A.P. and N.S.; software, P.S. and A.P.; validation, P.S. and N.S.; formal analysis, P.S., A.P. and N.S.; investigation, P.S. and AP; resources, P.S. and N.S.; data curation, A.P.; writing—original draft preparation, P.S. and A.P.; writing—review and editing, P.S. and N.S.; visualization, A.P. and P.S.; supervision, P.S.; project administration, P.S. and A.P.; funding acquisition, P.S. and A.P. All authors have read and agreed to the published version of the manuscript.

Funding: This research was financially supported by the KU Science Graduate Research Fund (GRF), Faculty of Science, Kasetsart University, and Kasetsart University for research funding through the Biodiversity Center Kasetsart University.

Data Availability Statement: The original contributions presented in this study are included in the article. Further inquiries can be directed to the corresponding author.

Acknowledgments: The authors gratefully acknowledge Ekaphan Kraichak for his valuable comments and assistance with data visualization.

Conflicts of Interest: The authors declare no conflicts of interest.

Abbreviations

The following abbreviations are used in this manuscript:

ASVs	Amplicon Sequence Variants
BKF	Forest Herbarium—BKF
CAM	Crassulacean Acid Metabolism
CITES	Convention on International Trade in Endangered Species
CPD	Critical Point Drying
DAPI	4′,6-diamidino-2-phenylindole
DNA	Deoxyribonucleic acid
dsDNA	Double-stranded DNA
DW	Distilled water
LM	Light microscope
PBS	Phosphate-buffered solution

PCR	Polymerase Chain Reaction
PE	Buffer PE
QC	Quality control
rRNA	Ribosomal RNA
SEM	Scanning Electron Microscope
TBE	Tris-Borate-EDTA
TEM	Transmission Electron Microscope

References

1. Freudenstein, J.V.; Chase, M.W. Phylogenetic relationships in Epidendroideae (Orchidaceae), one of the great flowering plant radiations: Progressive specialization and diversification. *Ann. Bot.* **2015**, *115*, 665–681. [CrossRef] [PubMed]
2. Averyanov, L.; Nguyen, K.; Maisak, T. *Chiloschista pulchella* (Orchidaceae: Aeridinae) new orchid species from Lao PDR. *Taiwania* **2018**, *63*, 389–392. [CrossRef]
3. Chanokkhun, T.; Jitpromma, T.; Muangsan, N.; Watthana, S. Notes on Phylogeny of the Genus *Chiloschista* Lindl. (Orchidaceae) in Thailand. *EasyChair Prepr.* **2023**. Available online: https://easychair.org/publications/preprint/xJChK/open (accessed on 19 April 2026).
4. Phelps, J.; Webb, E.L. "Invisible" wildlife trades: Southeast Asia's undocumented illegal trade in wild ornamental plants. *Biol. Conserv.* **2015**, *186*, 296–305. [CrossRef]
5. Suetsugu, K.; Sugita, R.; Yoshihara, A.; Okada, H.; Akita, K.; Nagata, N.; Tanoi, K.; Kobayashi, K. Aerial roots of the leafless epiphytic orchid *Taeniophyllum* are specialized for performing crassulacean acid metabolism photosynthesis. *New Phytol.* **2023**, *238*, 932–937. [CrossRef]
6. Cockburn, W. Tansley Review No 1. Variation in photosynthetic acid metabolism in vascular plants: CAM and related phenomena. *New Phytol.* **1985**, *101*, 3–24. [CrossRef]
7. Johnson, L.J.A.N.; Kane, M.E.; Zettler, L.W.; Mueller, G.M. Diversity and specificity of orchid mycorrhizal fungi in a leafless epiphytic orchid, *Dendrophylax lindenii* and the potential role of fungi in shaping its fine-scale distribution. *Front. Ecol. Evol.* **2023**, *11*, 1057940. [CrossRef]
8. Ramey, B.; Koutsoudis, M.; Bodman, S.; Fuqua, C. Biofilm Formation in Plant-Microbe Associations. *Curr. Opin. Microbiol.* **2005**, *7*, 602–609. [CrossRef]
9. Deepthi, A.S.; Ray, J.G. Algal associates and the evidence of cyanobacterial nitrogen fixation in the velamen roots of epiphytic orchids. *Glob. Ecol. Conserv.* **2020**, *22*, e00946. [CrossRef]
10. Tsavkelova, E.A.; Glukhareva, I.D.; Volynchikova, E.A.; Egorova, M.A.; Leontieva, M.R.; Malakhova, D.V.; Kolomeitseva, G.L.; Netrusov, A.I. Cyanobacterial Root Associations of Leafless Epiphytic Orchids. *Microorganisms* **2022**, *10*, 1006. [CrossRef]
11. Kumar, K.; Mella-Herrera, R.A.; Golden, J.W. Cyanobacterial heterocysts. *Cold Spring Harb. Perspect. Biol.* **2010**, *2*, a000315. [CrossRef]
12. Rai, A.N. Cyanobacteria in symbiosis. In *CRC Handbook of Symbiotic Cyanobacteria*; CRC Press: Boca Raton, FL, USA, 1990; Volume 1, pp. 1–7.
13. Thangavelu, M.; Kowsalya, A. Comparative anatomy of aerial and substrate roots of *Acampe praemorsa* (Rox.) Blatt. & McCann. *Flora* **2017**, *226*, 17–28. [CrossRef]
14. Grierson, C.; Nielsen, E.; Ketelaarc, T.; Schiefelbein, J. Root hairs. *Arab. Book* **2014**, *12*, e0172. [CrossRef] [PubMed]
15. Hoffmann, L.; Komárek, J.; Kaštovský, J. System of Cyanoprokaryotes (Cyanobacteria)—State in 2004. *Algol. Stud.* **2005**, *117*, 95–115. [CrossRef]
16. John, D.M.; Whitton, B.A.; Brook, A.J. *The Freshwater Algal Flora of the British Isles: An Identification Guide to Freshwater and Terrestrial Algae*; Cambridge University Press: Cambridge, UK, 2002.
17. Komárek, J. Cyanoprokaryota 2. In *Teil: Oscillatoriales. SuBwasserflora von Mitteleuropa*; Spektrum Akademischer Verlag: Heidelberg, Germany, 2005.
18. Strunecky, O.; Ivanova, A.P.; Mares, J. An updated classification of cyanobacterial orders and families based on phylogenomic and polyphasic analysis. *J. Phycol.* **2023**, *59*, 12–51. [CrossRef]
19. Wehr, J.D.; Sheath, R.G.; Kociolek, J.P. *Freshwater Algae of North America: Ecology and Classification*; Elsevier: Amsterdam, The Netherlands, 2015.
20. Guiry, M.D.; Guiry, G.M. AlgaeBase. Available online: https://www.algaebase.org (accessed on 3 April 2025).
21. Li, S.; Tan, H.; Liu, B.; Zhu, H.; Hu, Z.; Liu, G. Watanabeales ord. nov. and twelve novel species of Trebouxiophyceae (Chlorophyta). *J. Phycol.* **2021**, *57*, 1167–1186. [CrossRef]

22. Romac, S. Total DNA Extraction from Microalgae Strain Samples Using NucleoSpin Plant Modified Kit (Macherey Nagel). Available online: https://www.protocols.io/view/total-dna-extraction-from-microalgae-strain-sample-n92ldzbzxv5b/v1/metadata (accessed on 20 August 2025).
23. Lefler, F.W.; Berthold, D.E.; Laughinghouse, H.D., IV. Cyanoseq: A database of cyanobacterial 16S rRNA gene sequences with curated taxonomy. *J. Phycol.* **2023**, *59*, 470–480. [CrossRef]
24. Xu, P.; Li, X. Integrative Taxonomy in Algae Combining Morphological, Molecular, and Ecological Data for Species Delimitation. *Int. J. Mol. Evol. Biodivers.* **2024**, *14*, 186–196. [CrossRef]
25. Mateo, P.; Perona, E.; Berrendero, E.; Leganés, F.; Martín, M.; Golubić, S. Life cycle as a stable trait in the evaluation of diversity of Nostoc from biofilms in rivers. *FEMS Microbiol. Ecol.* **2011**, *76*, 185–198. [CrossRef]
26. Hoffmann, L.; Demoulin, V. Morphological variability of some species of Scytonemataceae (Cyanophyceae) under different culture conditions. *Bull. Société R. Bot. Belg.* **1985**, *118*, 189–197.
27. Jin, S.; Kim, K.Y.; Kim, M.-S.; Park, C. An assessment of the taxonomic reliability of DNA barcode sequences in publicly available databases. *Algae* **2020**, *35*, 293–301. [CrossRef]
28. Drobnitch, S.T.; Jensen, K.H.; Prentice, P.; Pittermann, J. Convergent evolution of vascular optimization in kelp (Laminariales). *Proc. Biol. Sci.* **2015**, *282*, 20151667. [CrossRef] [PubMed]
29. Tsavkelova, E.A.; Lobakova, E.S.; Kolomeitseva, G.L.; Cherdyntseva, T.A.; Netrusov, A.I. Localization of Associative Cyanobacteria on the Roots of Epiphytic Orchids. *Microbiology* **2003**, *72*, 86–91. [CrossRef]
30. Darlenko, T.; Pröschold, T. The genus *Jaagichlorella reisigl* (Trebouxiophyceae, Chlorophyta) and its close relatives: An evolutionary puzzle. *Phytotaxa* **2019**, *388*, 47–68. [CrossRef]
31. Arguelles, E. First Report of Microalgae Associated with Velamen Aerial Roots of Epiphytic Orchids in the Philippines: Microalgae in Velamen Roots of Orchids in the Philippines. *J. Trop. Life Sci.* **2025**, *15*, 223–234. [CrossRef]
32. Ram, A.T.; Shamina, M. Identification of cyanobacterial association from the roots of the terrestrial orchid, *Spathoglottis plicata* Blume. *Int. J. Adv. Res.* **2015**, *3*, 1477–1479.
33. Tsavkelova, E.A.; Cherdyntseva, T.; Lobakova, E.; Kolomeitseva, G.; Netrusov, A.I. Microbiota of the Orchid Rhizoplane. *Microbiology* **2001**, *70*, 492–497. [CrossRef]
34. Tsavkelova, E.A.; Lobakova, E.; Kolomeitseva, G.; Cherdyntseva, T.; Netrusov, A. Associative Cyanobacteria Isolated from the Roots of Epiphytic Orchids. *Microbiology* **2003**, *72*, 92–97. [CrossRef]
35. Whitton, B.; Potts, M. *The Ecology of Cyanobacteria: Their Diversity in Time and Space*; Springer: New York, NY, USA, 2002; Volume 1.
36. Büdel, B. Ecology and diversity of rock-inhabiting cyanobacteria in tropical regions. *Eur. J. Phycol.* **1999**, *34*, 361–370. [CrossRef]
37. Pridgeon, A.M.; Phillip, J.C.; Chase, M.W.; Rasmussen, F.N. Genera Orchidacearum Volume 3, Orchidoideae (Part 2), Vanilloideae. *Kew Bull.* **2003**, *59*, 140.
38. Zotz, G.; Winkler, U. Aerial roots of epiphytic orchids: The velamen radicum and its role in water and nutrient uptake. *Oecologia* **2013**, *171*, 733–741. [CrossRef] [PubMed]
39. Tay, J.Y.L.; Zotz, G.; Gorb, S.N.; Einzmann, H.J.R. Getting a Grip on the Adhesion Mechanism of Epiphytic Orchids—Evidence From Histology and Cryo-Scanning Electron Microscopy. *Front. For. Glob. Change* **2021**, *4*, 764357. [CrossRef]
40. Dycus, A.M.; Knudson, L. The role of the velamen of the aerial roots of orchids. *Bot. Gaz.* **1957**, *119*, 78–87. [CrossRef]
41. Sanford, W.W.; Adanlawo, I. Velamen and exodermis characters of West African epiphytic orchids in relation to taxonomic grouping and habitat tolerance. *Bot. J. Linn. Soc.* **1973**, *66*, 307–321. [CrossRef]
42. Moreira, A.S.; Isaias, R. Comparative anatomy of the absorption roots of terrestrial and epiphytic orchids. *Braz. Arch. Biol. Technol.* **2008**, *51*, 83–93. [CrossRef]
43. Mawinei, N.; Paramitha, Q. Comparative anatomy of roots and leaves in epiphytic and terrestrial orchids: Insights into adaptations and ecological strategies. *Law Econ.* **2024**, *18*, 73–85.
44. Leroux, O.; Bagniewska-Zadworna, A.; Rambe, S.K.; Knox, J.P.; Marcus, S.E.; Bellefroid, E.; Stubbe, D.; Chabbert, B.; Habrant, A.; Claeys, M.; et al. Non-lignified helical cell wall thickenings in root cortical cells of Aspleniaceae (Polypodiales): Histology and taxonomical significance. *Ann. Bot.* **2011**, *107*, 195–207. [CrossRef]
45. Hernández, M.A.; Terán, L.; Mata, M.; Martínez, O.G.; Prado, J. Helical cell wall thickenings in root cortical cells of Polypodiaceae species from northwestern Argentina. *Am. Fern J.* **2013**, *103*, 225–240. [CrossRef]
46. Porembski, S.; Barthlott, W. Velamen radicum micromorphology and classification of Orchidaceae. *Nord. J. Bot.* **1988**, *8*, 117–137. [CrossRef]
47. Zotz, G.; Schickenberg, N.; Albach, D. The velamen radicum is common among terrestrial monocotyledons. *Ann. Bot.* **2017**, *120*, 625–632. [CrossRef]
48. Idris, N.A.; Aleamotu'a, M.; McCurdy, D.W.; Collings, D.A. The orchid velamen: A model system for studying patterned secondary cell wall development? *Plants* **2021**, *10*, 1358. [CrossRef] [PubMed]
49. Idris, N.A.; Collings, D.A. Cell wall development in the velamen of the orchid *Miltoniopsis* investigated by confocal microscopy. *Malays. J. Microsc.* **2014**, *10*, 20–26.

50. Almeida, A.B.R.; Smidt, E.C.; Amano, E. Development and function of root hairs in *Acianthera* Scheidw. (Orchidaceae: Pleurothallidinae). *Aust. J. Basic Appl. Sci.* **2016**, *10*, 122–126.
51. Balachandar, M.; Muthukumar, T.; Ranjithamani, A.; Ravi, R.K. Comparative vegetative anatomy and mycorrhizal morphology of three South Indian *Luisia* species (Orchidaceae) with the note on their epiphytic adaptations. *Flora* **2019**, *251*, 39–61. [CrossRef]
52. Balachandar, M.; Muthukumar, T.; Nagaraj, K.; Ravi, R.K. Vegetative anatomy and mycorrhizal morphology of *Schoenorchis nivea* (Lindl.) Schltr., (Orchidaceae) and their adaptive significance. *Acta Biol. Szeged.* **2019**, *63*, 1–13. [CrossRef]
53. Rasmussen, A.; Dobrijevic, D.P.; Ola, A.; Ishaya, F.D.; Lovelock, C.E. Aerial Root Physiology: Reaching for the Sky or Down to Earth? *Annu. Plant Rev. Online* **2019**, *2*, 753–784.
54. Chomicki, G.; Bidel, L.P.; Jay-Allemand, C. Exodermis structure controls fungal invasion in the leafless epiphytic orchid *Dendrophylax lindenii* (Lindl.) Benth. ex Rolfe. *Flora* **2014**, *209*, 88–94. [CrossRef]
55. Geldner, N. The endodermis. *Annu. Rev. Plant Biol.* **2013**, *64*, 531–558. [CrossRef]
56. Hose, E.; Clarkson, D.T.; Steudle, E.; Schreiber, L.; Hartung, W. The exodermis: A variable apoplastic barrier. *J. Exp. Bot.* **2001**, *52*, 2245–2264. [CrossRef]
57. Doblas, V.G.; Geldner, N.; Barberon, M. The endodermis, a tightly controlled barrier for nutrients. *Curr. Opin. Plant Biol.* **2017**, *39*, 136–143. [CrossRef]
58. Zhang, S.; Yang, Y.; Li, J.; Qin, J.; Zhang, W.; Huang, W.; Hu, H. Physiological diversity of orchids. *Plant Divers.* **2018**, *40*, 196–208. [CrossRef]
59. Du, J.; Guo, S.; Li, X.; Geng, Z.; Yuan, Z.; Song, X. Study on the Rhizosphere Soil Microbial Diversity of Five Common *Orchidaceae* Species in the Transitional Zone Between Warm Temperate and Subtropical Regions. *Diversity* **2025**, *17*, 605. [CrossRef]

Disclaimer/Publisher's Note: The statements, opinions and data contained in all publications are solely those of the individual author(s) and contributor(s) and not of MDPI and/or the editor(s). MDPI and/or the editor(s) disclaim responsibility for any injury to people or property resulting from any ideas, methods, instructions or products referred to in the content.